Influence of submodel size and evaluated functions on the optimization process of crashworthiness structures

Simon Link, Harman Singh, Axel Schumacher

University of Wuppertal, Faculty for Mechanical Engineering and Safety Engineering,
Chair for Optimization of Mechanical Structures, Gaußstraße 20, 42119 Wuppertal, Germany

1 Introduction

Optimization of crashworthiness structures is an influential aspect during the development of a vehicle body. Structural optimization is a procedure to enhance the mechanical properties of a structure through changing the geometry like the size, shape or topology. This paper deals with the structural optimization of large crashworthy systems with modifications to their shape and topology using a submodel technique. The submodel technique is incorporated into a multilevel optimization procedure [1] using two levels, where level 1 is the large system und level 2 is a submodel of the large system. The optimization is carried out in level 2 using different submodel sizes. Furthermore the influence of updating the boundary conditions on the evaluated functions of level 1 and level 2 has been studied. Research has been done on how to select the submodel, what type of boundary conditions are required in the submodel, when these boundary conditions should be updated, which evaluated functions should be used in the submodel and what is the saving in computation time using a submodel in the optimization. The research is demonstrated using two applications, a cantilever frame impacted by a rigid sphere and a rocker beam in a pole impact load case.

2 Multilevel techniques

2.1 Submodel technique

A submodel is a region of interest cut out from a large system which is to be analyzed in detail. To simulate a submodel, time dependent boundary conditions are required at the interfaces where the submodel region is cut out. These boundary conditions are extracted during an analysis of the large system and can be displacements or forces of nodes at the interfaces (nodal interface boundary conditions). These interface boundary conditions can also be defined by other physical quantities depending on the problem. If the boundary conditions are exact, the submodel region will deform identical to the deformation of this region in the large system. In order to maintain the same mechanical behavior of the submodel region as compared to the same region in the large system, an update of the boundary conditions is required during the optimization process. This submodeling technique can be used in the optimization process for different hierarchical levels as shown in figure 1.
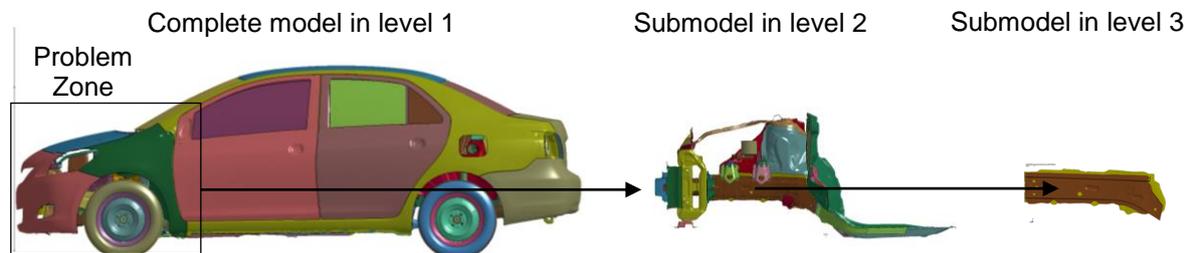
Fig.1: *Submodeling technique shown using a Toyota Yaris FE-Model for front crash [2]*

2.2 Influence of submodel size and evaluated functions

The size of the submodel region and the update of the boundary conditions play a significant role in the optimization process and can also have a negative influence on the optimization results. On the other hand, the main advantage of the submodel technique is the smaller size of the submodel, which

leads to a reduction of computation time, the usage of less computer storage space and the possibility to use a finer mesh for higher resolution of critical areas.

In order to improve the design of large structures, optimization in different levels can be used. For example, level 1 is the large system and level 2 is a submodel of the large system. Both levels are coupled together with the help of interface functions to form a multilevel optimization process using the submodel technique. Thereby it is important to use an appropriate objective and constraint function in the submodel. The function used as an interface boundary condition in the submodel remains unchanged during one complete iteration. Hence this function cannot be used as objective or constraint in that iteration of submodel optimization. Therefore a correlation of different possible objective or constraint functions in level 1 is necessary in order to choose a useful objective function for the submodel optimization in level 2. The correlation can be a linear or non-linear relationship. In this research only linear correlation is considered. If x and y represent a dataset containing n values to be correlated, then according to Pearson [3], if the correlation coefficient r_{xy} has a value of +1, it means x and y share a total positive linear correlation and if the value of r_{xy} is -1 it means they share a total negative linear correlation. Whereas, if the calculated value of r_{xy} is 0, it means there is no correlation between x and y at all.

This type of correlation analysis is used to study the relationship between various structure responses. If the objective function in each level is different, the correlation analysis is necessary. Only if the objective functions correlate, they can be replaced by each other in the multilevel optimization. The correlation analysis will be shown on two different applications for crash in this research work.

2.3   Multilevel optimization workflow

The multilevel optimization workflow for two levels is shown in figure 2. At first there is a start design in level 1, which is a complete model. This complete model is analyzed and then evaluated for the desired objective functions in level 1. If the stop criterion is not reached, the design variables are changed and the outer loop is repeated. The stop criteria can be, for example, the maximum number of iterations or a criterion for the convergence of the solution.
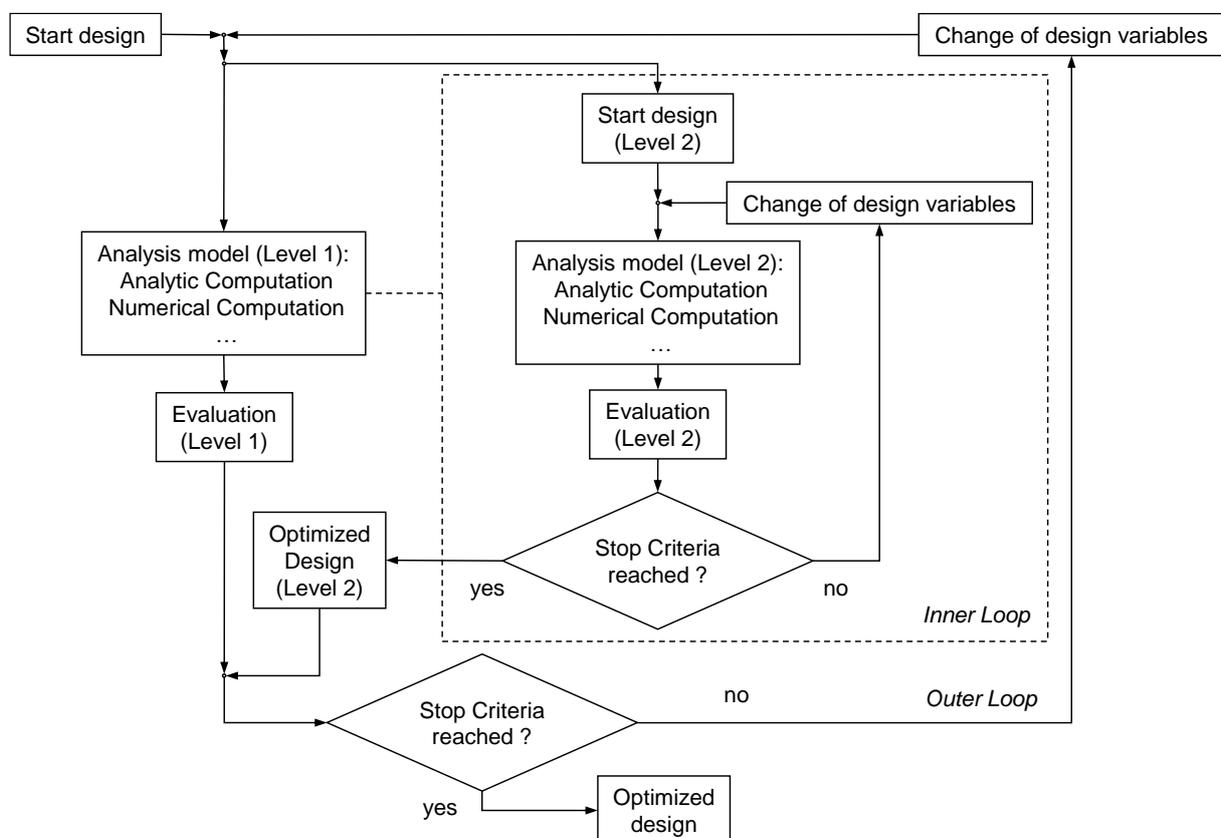
Fig.2:   Multilevel optimization workflow, modified [1]

For each iteration in level 1, an inner loop is performed which is defined as level 2. The design parameters of level 1 are transferred and integrated into level 2. The start design in level 2 is a

submodel of the complete model. The submodel is then analyzed based on the information extracted from level 1. The objective functions of level 2 are then evaluated and the inner loop is repeated until a stop criterion in level 2 is reached. Once the optimization in the inner loop is finished, the optimized design of level 2 is integrated into level 1. All these new designs from the outer loop in level 1 are then finally evaluated and at the end an optimized design is given out.

The type of analysis in each level can be defined by the user itself. The design variables, constraints and objective functions can be different for each level depending on the problem. If the structure response used in each level is different, then a correlation of these structure responses is mandatory, in order to run the multilevel optimization successfully.

3 Application 1: Cantilever frame impacted by a rigid sphere

3.1   Problem description

A cantilever frame of mass 38 g is fixed at one side and is impacted by a rigid sphere of mass 1 kg with a velocity of 28 km/h as shown in figure 3. The cantilever is made of an aluminum sheet of size 150 mm x 100 mm and a thickness of 0.6 mm, which is surrounded by an aluminum frame of 10 mm width and 1 mm thickness. The aluminum sheet is divided in two parts, the outer and the inner portion. The inner portion is a square of size s containing a semicircular bead of length L_s and radius R_s in its center, whereas the outer portion connects the frame to the inner portion. The position of the inner portion is controlled by the variables X_s and Y_s.
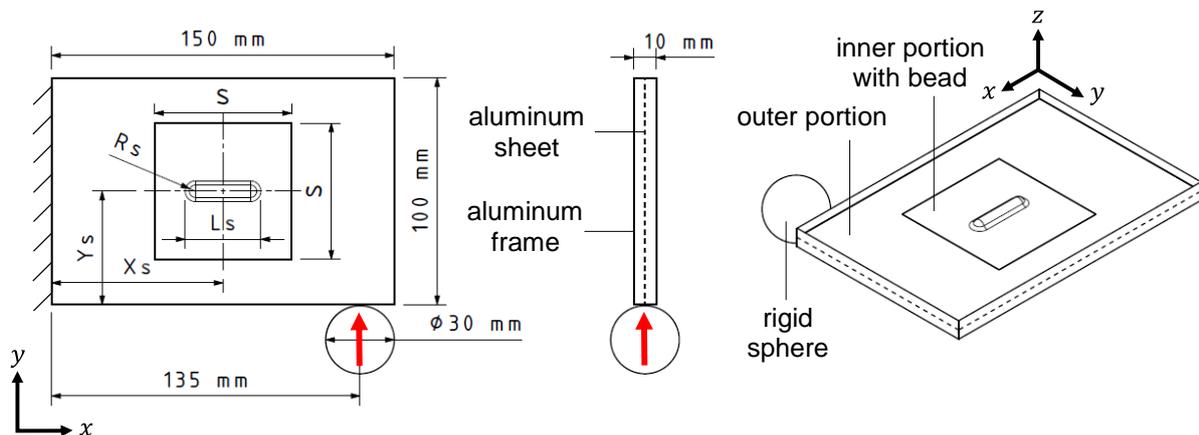
Fig.3:   *An aluminum cantilever frame impacted by a rigid sphere*

The intrusion of the sphere is calculated using the *Finite-Element-Method* in *LS-DYNA®* solver with an explicit time integration. The cantilever model is meshed with an element size of 1.5 mm and the shell element formulation of Belytschko-Tsay. The sphere is meshed with tetrahedral volume elements and consists of a rigid material of an artificial density 10 times the density of steel. Figure 4 compares the simulation results of the cantilever frame without the bead to the initial design with bead, where $X_s = 75$ mm, $Y_s = 50$ mm, $L_s = 20$ mm, $R_s = 3$ mm and $s = 60$ mm.
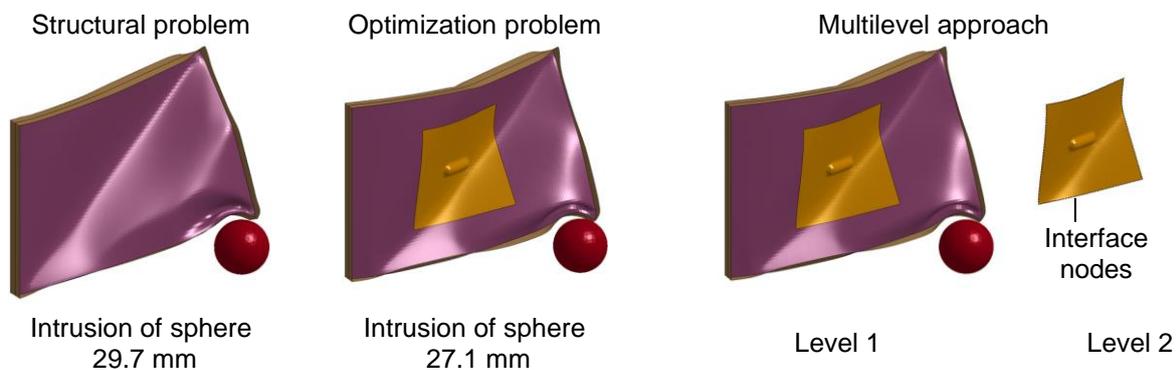
Fig.4:   *Simulation results of the initial design of the cantilever frame with and without the bead and the multilevel approach to solve the optimization problem*

As shown in figure 4, the intrusion of the sphere in the cantilever frame without bead is 29.7 mm, whereas the intrusion in the initial design with the bead is 27.1 mm. The simulation results show that the cantilever frame deforms locally were the rigid sphere hits the frame. There is also a global diagonal buckling in the frame, which is more critical. The consequence of the buckling is the high intrusion of the rigid sphere into the structure. The buckling of the cantilever frame can be reduced by increasing its stiffness. To achieve this, one possibility is to change the position and the dimensions of the bead inside the cantilever frame. Therefore, the optimization task is to decrease the intrusion of the sphere by changing the variables X_s, Y_s, L_s and R_s, where the constraint is to stop the rigid sphere in y-direction.

The multilevel approach of this optimization problem is shown in figure 4 using two levels. Level 1 is the complete model of the cantilever frame and level 2 is the submodel of the cantilever frame. This submodel is the inner square portion of size s cut out from the cantilever frame and comprises of the bead and its surrounding. The interface function is the time dependent nodal displacements of the interface nodes. It is extracted from the simulation of level 1 and prescribed for the submodel in level 2. In case of submodel size *s = 60 mm*, the time required for running the FE-simulation of the submodel is only 15% of the time required for the complete model. Therefore a high number of function calls can be performed in level 2 compared to level 1, in a given period of time and depending on the submodel size.

3.2   Correlation analysis for the cantilever frame optimization problem

The correlation of objective functions is a very important aspect in the multilevel optimization problem. The objective in level 1 is the intrusion of the rigid sphere and in level 2 it is the internal energy of the submodel.
The internal energy of the submodel is chosen for two reasons. Firstly, there is no rigid sphere in level 2, therefore the intrusion of rigid sphere cannot be used as objective function. Secondly, the nodal displacements are used as interface functions in the submodel, which remain the same during the submodel optimization. Thus, in order to increase the stiffness of the cantilever frame, either the forces or the internal energy in the submodel can be used as appropriate objective function. In this current work, internal energy has been chosen as an objective function, however in future research other types of objective functions will be studied and correlated.
The two objective functions intrusion and internal energy are evaluated in the complete model using 1000 sampling points as shown in figure 5. According to Pearson [3], the correlation coefficient between these two objective functions is found to be -0.89. The negative value means a negative linear correlation, i.e. in order to reduce the intrusion of rigid sphere, the internal energy of the submodel has to be increased.
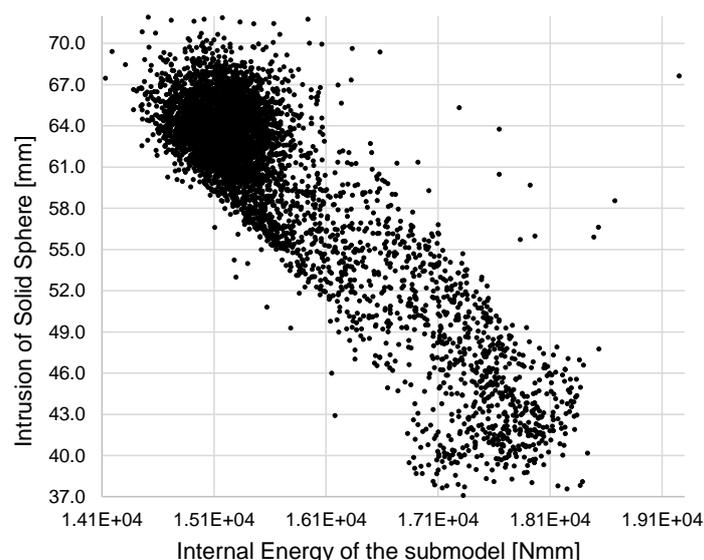
Fig.5:   Correlation of intrusion of rigid sphere and internal energy of submodel for cantilever frame

It is also important here to mention the outliers in figure 5. There are only a few sampling points which lie outside the central data cloud. These outlier points may have a bad influence on the correlation values. Another aspect in the correlation analysis is the range of samples, which means for a particular value of the internal energy in the submodel, there might be numerous samples having a wide range of intrusion values. The influence of the outliers and the range of correlating samples will be studied in detail in future research.

3.3   Multilevel optimization setup and results

Table 1 shows the selection of the objective functions and constraints during the optimization of the cantilever frame. As already discussed in the correlation analysis, the goal in level 1 is to minimize the intrusion of the rigid sphere in y-direction. To achieve this goal, the internal energy of the submodel is maximized in level 2. In this academic example there are no manufacturing constraints specified for both levels. To fulfil the functional constraint in level 1, the end velocity of the rigid sphere in y-direction has to be less than zero by the end of the simulation.

Objective level 1:	Minimize the intrusion of the rigid sphere in y-direction
Functional constraint level 1:	The end velocity of the sphere in y-direction < 0 mm/s
Objective level 2:	Maximize the internal energy of the submodel
Functional constraint level 2:	None
Manufacturing constraint:	None

Table 1:   Objective function and constraints for the Multilevel Optimization of cantilever frame

The design variables for each level are shown in Table 2 along with their upper and lower limits. In level 1 the position of the bead in x- and y-direction (X_s, Y_s) and in level 2 the length (L_s) and the radius (R_s) of the bead are varied. The design exploration in level 1 is a design of experiments (DOE), where 12 sampling points are chosen using the adjustable full factorial. For each sampling point of level 1 (outer loop), a submodel optimization is started in level 2 (inner loop), using a differential evolution algorithm with total 40 iterations. Hence, total 480 function calls are made during the multilevel optimization. In case of multilevel optimization without submodel, the complete model of the cantilever frame is used in both levels and the objective function in both levels is to reduce the intrusion of the rigid sphere.

The multilevel optimization was carried out for two different submodel sizes. A smaller submodel of size s = 40 mm and a larger submodel of size s = 60 mm. The results are shown in table 2 and figure 6. It is figured out that the bead position in both cases was different, whereas the length and the radius of the bead in both cases tends to the upper limit during the optimization. The larger submodel shows better results in comparison to the smaller submodel.
The intrusion of the rigid sphere in case of the smaller submodel is 22.82 mm and in case of the larger submodel it is 19.51 mm. These results were compared to the results of the multilevel optimization without the submodel technique, where the intrusion of the rigid sphere is 18.86 mm. The result of the optimization without the submodel is better than the result with the larger submodel. However this gap is small and could be eliminated by improving the submodeling technique in further researches.

	Level	Variable name	Start value	Lower limit	Upper limit	Optimized values for smaller submodel (s = 40)	Optimized values for larger submodel (s = 60)	Optimized values without submodel
Design variables	1	Position X_s	75 mm	36 mm	114 mm	62 mm	62 mm	62 mm
		Position Y_s	50 mm	36 mm	64 mm	36 mm	50 mm	36 mm
	2	Bead Length L_s	20 mm	10 mm	30 mm	29.96 mm	29.96 mm	28.21 mm
		Bead Radius R_s	3 mm	2 mm	5 mm	4.84 mm	4.84 mm	2.67 mm
Objective function	1	To minimize the solid sphere intrusion				**22.82 mm**	**19.51 mm**	**18.86 mm**
	2	To maximize the internal energy of submodel				**1080 Nmm**	**1455 Nmm**	**1393 Nmm**

Table 2:   Results of the multilevel optimization
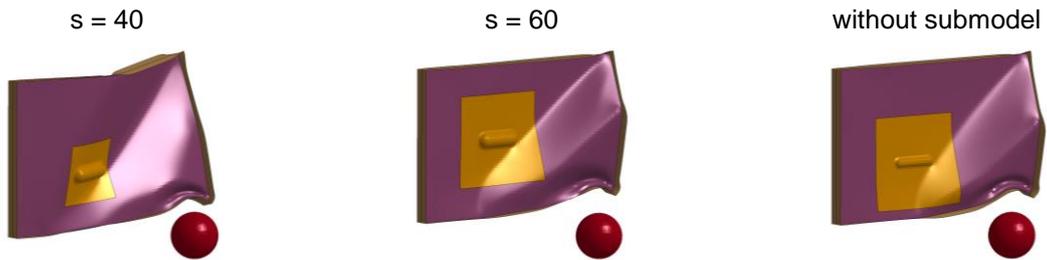
Fig.6:   Comparison of optimized designs with and without using submodel in the optimization

It is also found that the complete elimination of the buckling might not be possible as shown in figure 6. However by changing the position and size of the bead, the mechanical behavior of the cantilever frame can be changed drastically. On the other hand the time saved using the submodel technique is enormous. Table 3 shows the comparison of total time required for 480 function calls in case of multilevel optimization with and without using the submodel. It should also be considered that an optimization without a submodel might require less function calls.

Total no. of functions calls	Multilevel optimization with submodel size s = 40	Multilevel optimization with submodel size s = 60	Multilevel Optimization without submodel	Time saved % (In comparison to s = 60)
480	4 hours 11 minutes	4 hours 54 minutes	22 hours 56 minutes	18 hours 2 mins (78.6 %)
LSDYNA Simulation using SMP 4 x Intel(R) Core(TM) i7-4770 CPU @ 3.40GHz				

Table 3:   Comparison of total time required by the optimization in all three cases

4 Application 2: Rocker beam in a pole impact load case

4.1   Problem description

The simulation model in figure 7 shows a section of an aluminum rocker beam of a vehicle, which is connected to a part of the seat cross-member and moves with an initial velocity of 29 km/h into the direction of a rigid pole. A rigid wall of mass 85 kg with the same velocity is connected to the end of the cross-member to increase the impact energy. The length of the rocker beam is 600 mm.
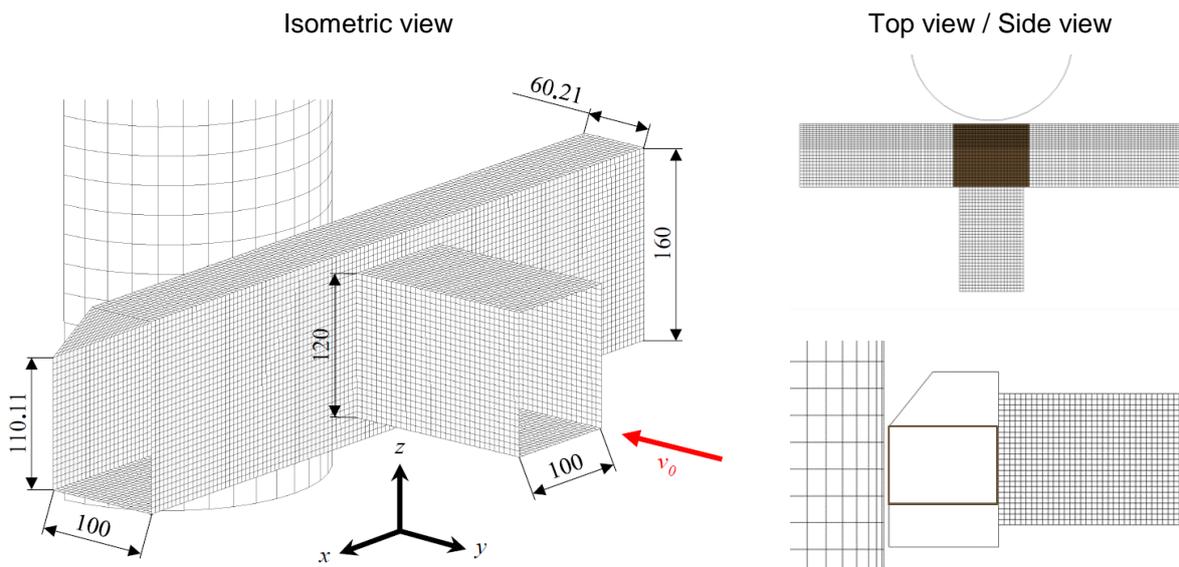
Fig.7:   Isometric view, top view and side view of the simulation model - inlay marked brown, modified [4]

This model is only a part of a complete vehicle, so boundary conditions have to be used to achieve a similar behavior of the structure as in the complete vehicle. For this purpose, all degrees of freedom of

the FE-nodes of the cross-member, which adjoin the rigid wall, are restricted except for the y-translation. In addition, the z-translation of the FE-nodes of the outer rows of the rocker beam, which are facing the pole, must be restricted [4].

The intrusion denotes the maximum value of the indentation in the rocker beam. This is determined by the maximum y-displacement of the rigid wall (minus the initial gap between the rocker beam and the pole), which is positioned at the end of the seat cross-member.

An aluminum inlay (brown marked in figure 7) is integrated in the rocker beam, in order to increase the local stiffness of the structure. These inlays are used for example in crash structures of vehicles where a local increase in stiffness is desired. The position of the inlay in the rocker beam and its overlap with the pole is shown in figure 7. The inlay is positioned in the middle of the rocker beam, such that all components share the same symmetry in the y-z plane. It is centrally located in front of the seat cross-member to evenly distribute the force induced by the seat cross-member. The inlay is the structure which is being optimized in this application. The Finite Element Analysis of this structural problem is carried out with LS-DYNA® solver using explicit time integration.

4.2 Optimization process and linking of level 1 and 2

In this application the optimization problem is divided in two levels. Level 1 contains the complete model of the rocker beam and level 2 comprises the submodel. This research is limited to an optimization with changes to the topology and shape of the inlay in level 2. No optimizations are performed in level 1. Level 1 is used to integrate the submodel into the complete model and extract the interface boundary conditions (here: nodal displacements) which are required to simulate the submodel. The linking of level 1 and 2 is implemented by these coupling boundary conditions, the objective function and constraints. The optimization is carried out with the "Graph and heuristic based topology optimization" (GHT) [4][5].

A query is added at the beginning of every iteration to determine whether the coupling boundary conditions should be updated. This can be for example necessary if the mechanical behavior of the submodel changes due to structural changes and the value of the objective function in the submodel deviates too much from level 1. An update of the coupling boundary conditions takes place according to the objective function values of the best design of the last iteration in level 2. This 'best design' is integrated in the complete model in level 1 and the simulation is performed to extract the new coupling boundary conditions. On the basis of these new boundary conditions the designs of the current iteration are evaluated in level 2. If no update of the interface boundary conditions is desired, the interface boundary conditions of the last iteration will be used. An update of the interface boundary conditions is always necessary in the first iteration, because otherwise no simulation of the submodel is possible.

Afterwards a loop runs over the best competing designs from the last iteration. The number of these designs can be defined by the user. By default the best 5 designs are transferred to the next iteration, whereas in iteration 1 only the start design is used. Then a heuristic for changing the topology is applied on each of the competing designs. This is done until every heuristic has been applied once on every competing design, which generates new designs for the current iteration. In addition the heuristics for changing the shape and the wall thickness are applied to these new generated designs. This procedure consists of smoothing the designs and scaling the wall thicknesses to fulfill the mass constraint. All the new designs are evaluated in level 2. If an improvement compared to the last iteration could be achieved, the next iteration starts. When no better design can be found, a shape optimization (and possibly a dimensioning) takes place with the best design of the last iteration.

Objective level 1:	Minimize the intrusion of the rocker beam
Functional constraint level 1:	Mass inlay = 330g
Objective level 2:	Maximize the internal energy of the inlay
Functional constraint level 2:	Mass inlay = 330g
Manufacturing constraint:	1.0 mm ≤ Wall thickness of the structure ≤ 3.5mm
	Connecting angle between two walls ≥ 15°
	Distance between two walls ≥ 10mm
	Ratio of biggest to smallest chamber ≤ 20

Table 4: Objective function and constraints of the optimization problem

The objective function in level 1 is to minimize the intrusion of the rocker beam. In order to achieve this objective in level 1, the internal energy of the inlay is maximized in level 2. The reason to choose internal energy is because a smaller intrusion leads to a higher stiffness of the inlay. Due to this the inlay will convert a higher fraction of the kinetic energy of the system into internal energy. The objective and constraints of the optimization problem are shown in table 4.

4.3 Correlation analysis for the rocker beam optimization problem

The correlation between the objective functions in level 1 and 2, internal energy and intrusion respectively, has been determined with the data of an optimization in level 1. Therefore, the values of internal energy and intrusion of all designs of the optimization are used as shown in figure 8. Due to this a good coverage of the design space with many different topology changes of the structure can be achieved. According to Pearson, the correlation coefficient of internal energy and intrusion is -0.95. This coefficient value denotes a very high correlation. Thus the internal energy of the inlay is suitable to replace the objective function intrusion in this optimization problem.
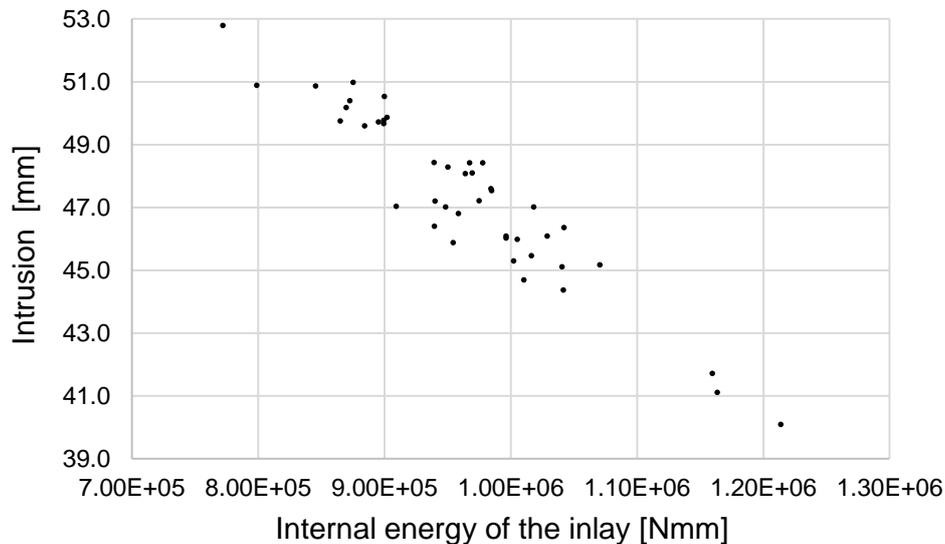
Fig.8: Correlation of intrusion of rocker beam and internal energy of inlay

4.4 Introduction of different submodels used in the optimizations

Figure 9 shows a comparison of three different submodels used in the optimizations. The small submodel only comprises the inlay on which the topological changes are applied. The interface boundary conditions are applied on the coupling nodes on the complete outer surface of the inlay, but not on the structure inside the inlay which is generated due to the topological changes.

In the medium submodel the complete cross-section of the rocker beam is included over a length of 130 mm. In addition the medium submodel comprises a small piece of the seat cross-member. No interface boundary conditions are applied on the inlay. The interface boundary conditions are applied on the coupling nodes on the cut surface of the rocker beam and the seat cross-member. The coupling nodes are marked white.

The large submodel is a modified version of the medium submodel. The length of the rocker beam is 250 mm and almost twice as long as the section of the rocker beam in the medium submodel. The part of the seat cross-member remains unchanged. The coupling nodes are marked white. They are located on the cut surface of the rocker beam and the seat cross-member. The number of coupling nodes is identical in the medium and the large submodel. In the submodels the same nodal displacements, nodal velocities and internal energies are generated as compared to the complete model.

Small submodel   Medium submodel   Large submodel
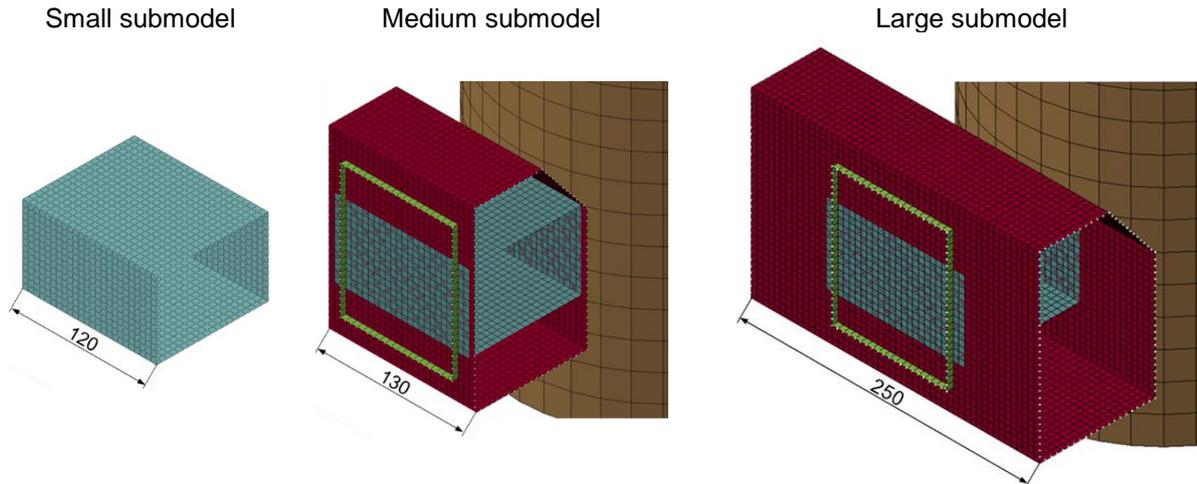
Fig.9: Different submodel sizes – rocker beam (red), seat cross-member (green), inlay (turquoise), rigid pole (brown), coupling nodes (white)

4.5   Optimization results

Two different types of investigations are performed to check whether the updated boundary conditions have an influence on the optimization process. In the first investigation, an optimization is carried out without updating the boundary conditions in each iteration. The interface boundary conditions are only updated in the first iteration. In the second investigation, the interface boundary conditions are updated in each iteration.

Figure 10 shows a comparison of the optimization history for both investigations. Furthermore, these investigations were done using different submodel sizes. The best design of every iteration which is evaluated by the objective function in level 2 is shown in figure 10. These best designs are compared to the results of the optimization in level 1, "reference internal energy", where the objective function was maximizing the internal energy of the inlay.

All the designs were evaluated in level 1 to measure the intrusion. In addition the mathematical graph of the inlay of the best design of each optimization is shown, which also describes the structure of the inlay. All designs of the inlay have a constant cross-section along the extrusion direction. The rigid pole is located on the right side of the mathematical graph of the inlay.
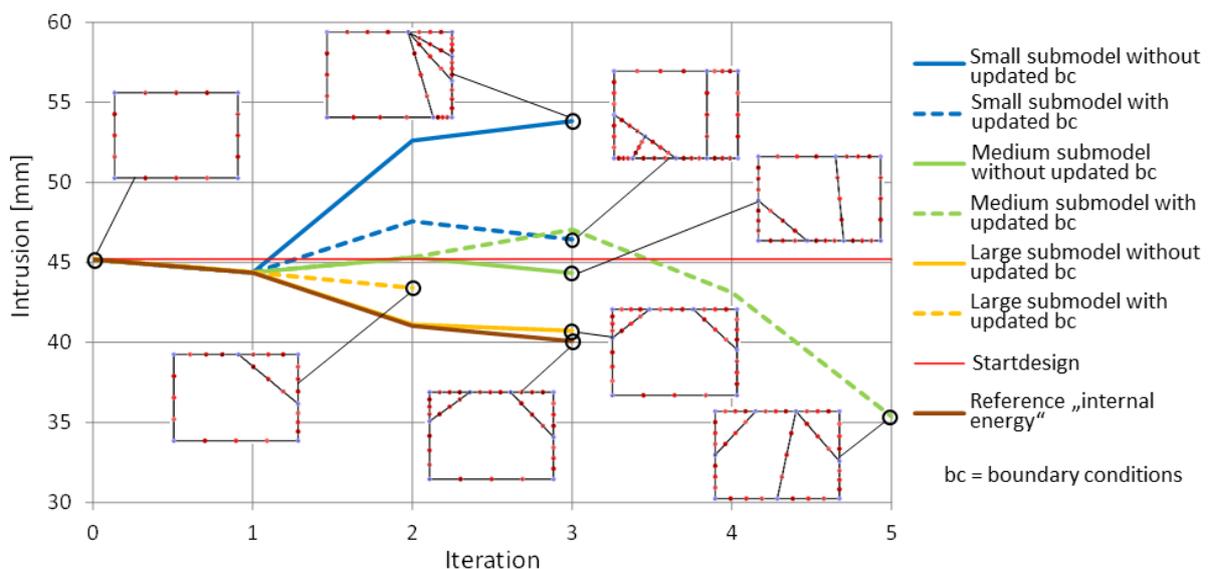
Fig.10: Optimization history of all submodels related to the intrusion

The "small submodel" cannot achieve an improvement of the intrusion compared to the value of the start design. Nevertheless the optimization with updated boundary conditions achieves better results for the small submodel in comparison to not updating the boundary conditions.

The final design of the optimization with the "medium submodel" with updated boundary conditions can achieve a significant improvement of the intrusion. This improvement is almost twice as good as the improvement in the reference optimization without submodel technique. During the optimization with the medium submodel, there is no improvement in the intrusion until the third iteration. However, the best designs in the iteration 4 and 5 show a significant reduction in intrusion. In this case it was possible to skip a local minimum in the reference optimization in level 1 which happens due to the evaluation of the designs in the submodel. This illustrates how different the designs can be evaluated in the submodel.

The large submodel generates designs with a continuous improvement of the intrusion in every iteration. Without updated boundary conditions almost the same final design is found as in the reference optimization in level 1. The optimization of the large submodel with updated boundary conditions stops after the second iteration, because no design with a higher internal energy could be found. This happens because the designs in the second iteration in level 1 are evaluated worse than they actually are. In this case the update of the coupling boundary conditions leads to a poorer optimization results compared to the results of the optimization without updated boundary conditions. The size of the submodel has a great influence on the optimization result, whereby the most reliable results can be achieved by the large submodel.

The larger the submodel and the greater the distance of the coupling nodes to the optimized structure, the smaller the influence of the coupling boundary conditions on this structure. Thus a larger submodel is more tolerant to changes in the topology of the structure and can adapt to changes of the stiffness better than a small submodel. Particularly, this is evident in the small submodel where the coupling nodes are directly applied on the inlay. Thus a change in the stiffness of the submodel structure cannot be taken into account in the optimization process.

A disadvantage of this simulation model is that there are almost no deformations on the seat cross-member. Because of this the displacements of the coupling nodes of the seat cross-member are directly applied on the inlay and an adaption to the change in stiffness of the inlay is not possible. With a submodel which does not apply the displacement boundary conditions directly on the structure to be optimized, better results can be achieved.

There is always a deviation in the mechanical behavior of a design, when simulated in the submodel using the coupling boundary conditions based on a different design. This phenomena can occur in both cases of updated and not updated boundary conditions, because these boundary conditions refer to a design with different mechanical properties. Hence an update of the boundary conditions might not always lead to a more precise evaluation of the designs in the submodel, which is seen in the optimization with the large submodel.

At last, the computation time, the required disk space and the number of finite elements of three different submodels are compared to the complete model in level 1. As shown in table 5, it is possible to save up to 60-70% of the computation time using submodels that are valid for GHT.

Model	Computation time (1 CPU) [s]	Disk space [MB]	Number of finite elements	Computation time related to complete model [%]
Complete model (Reference)	238	250	18962	-
Small submodel	11	24	1701	4.6
Medium submodel	69	89	6251	29.0
Large submodel	99	106	8627	41.6

Table 5: Comparison of computation time, disk space and number of finite elements of different submodel sizes

4.6   Problems of submodel optimization with GHT

GHT uses for example relative displacements of FE-nodes in the heuristics in order to determine the topological changes in the structure. So if the mechanical behavior of the submodel changes due to the simulation with or without updated boundary conditions, the topological changes GHT applies on the structure can be different. Thus the maximum potential of the heuristics could not be used in case

of submodel optimization. It should also be considered that the heuristics for shape and topology change use the data of the FE calculation from the last iteration. An update of the boundary conditions therefore has an influence on the heuristics in the subsequent iteration. This means that the designs of all submodels generated by the heuristics in the first and second iteration are identical. Regardless whether or not the boundary conditions are updated in the second iteration. Although the time to create a submodel has to be considered.

5 Conclusion

Submodel optimizations were carried out with different submodel sizes in both applications. The larger submodels achieved better results in both optimization problems of this research. This happens due to the larger distance between the coupling nodes and the optimized structure. Because of this the stiffness of the submodel can be considered more precisely.

Nodal displacements have been used as interface boundary conditions in the submodel. It is also possible to use other physical quantities like nodal forces as interface boundary conditions, which is still under research.

An important point in the submodel optimization is the update of the interface boundary conditions. When the deviation of the objective function of a design between level 1 and level 2 is inadmissibly high, an update of the interface boundary conditions is necessary. However, an update of the interface boundary conditions must not lead to a better optimization result in every case. In one particular case in the second application an update of the interface boundary conditions achieved poor results in comparison to an optimization without updated boundary conditions. This demonstrates the big influence of the interface boundary conditions during the evaluation of the designs in the submodel.

Another critical aspect is the selection of the evaluated functions for different levels in the optimization. If the evaluated function is not the same in each level, then a function with a high correlation to the original evaluated function should be used. The criteria to select these functions can be for example the correlation coefficient.

The submodel optimization has a huge potential to reduce the simulation cost. In this research it was possible to save up to 60-80% of the computation time with the use of submodels in the optimization.

6 Acknowledgement

7 Literature

[1]   Schumacher, A. (2013): "Optimierung mechanischer Strukturen", 2. Auflage, Springer Verlag, ISBN: 978-3-642-34699-6

[2]   TOYOTA YARIS MODEL (NCAC V01) http://www.ncac.gwu.edu/vml/models.html

[3]   Wang, J. (2013): "Encyclopedia of Systems Biology", Springer Verlag, ISBN: 978-1-4419-9863-7

[4]   Ortmann, C. (2015): "Development of a graph and heuristic based method for the topology optimization of crashworthiness profile structures", Shaker Verlag, ISBN: 978-3-8440-3746-3

[5]   Ortmann, C.; Schumacher, A. (2013a): "Graph and heuristic based topology optimization of crash loaded structures", Struct Multidisc Optim 47(6); 839-854